The *Cryptococcus neoformans* Rim101 Transcription Factor Directly Regulates Genes Required for Adaptation to the Host

Teresa R. O'Meara,[a] Wenjie Xu,[b] Kyla M. Selvig,[a] Matthew J. O'Meara,[c] Aaron P. Mitchell,[b] J. Andrew Alspaugh[a]

Departments of Medicine and Molecular Genetics and Microbiology, Duke University School of Medicine, Durham, North Carolina, USA[a]; Department of Biological Sciences, Carnegie Mellon University, Pittsburgh, Pennsylvania, USA[b]; Department of Computer Science, University of North Carolina—Chapel Hill, Chapel Hill, North Carolina, USA[c]

The Rim101 protein is a conserved pH-responsive transcription factor that mediates important interactions between several fungal pathogens and the infected host. In the human fungal pathogen *Cryptococcus neoformans*, the Rim101 protein retains conserved functions to allow the microorganism to respond to changes in pH and other host stresses. This coordinated cellular response enables this fungus to effectively evade the host immune response. Preliminary studies suggest that this conserved transcription factor is uniquely regulated in *C. neoformans* both by the canonical pH-sensing pathway and by the cyclic AMP (cAMP)/protein kinase A (PKA) pathway. Here we present comparative transcriptional data that demonstrate a strong concordance between the downstream effectors of PKA and Rim101. To define Rim101-dependent gene expression during a murine lung infection, we used nanoString profiling of lung tissue infected with a wild-type or *rim101Δ* mutant strain. In this setting, we demonstrated that Rim101 controls the expression of multiple cell wall-biosynthetic genes, likely explaining the enhanced immunogenicity of the *rim101Δ* mutant. Despite its divergent upstream regulation, the *C. neoformans* Rim101 protein recognizes a conserved DNA binding motif. Using these data, we identified direct targets of this transcription factor, including genes involved in cell wall regulation. Therefore, the Rim101 protein directly controls cell wall changes required for the adaptation of *C. neoformans* to its host environment. Moreover, we propose that integration of the cAMP/PKA and pH-sensing pathways allows *C. neoformans* to respond to a broad range of host-specific signals.

Microorganisms adapt to the stressful conditions of the infected host by translating stimuli from multiple signal transduction cascades into a coordinated cellular response. These signal transduction cascades can be activated by a number of host environmental stimuli, including high temperature, host physiological pH, and nutrient limitation (1). In *Cryptococcus neoformans*, these stimuli induce the expression of several virulence-associated phenotypes that allow this pathogenic fungus to survive in the host and cause disease. One important virulence factor is the polysaccharide capsule, which is the primary method of avoiding the host immune response and allowing effective survival within the host (2–6). Encapsulation requires increased polysaccharide biosynthesis, secretion of this polysaccharide across the cell wall, and remodeling of the cell wall to allow capsule attachment and maintenance around the cell (2, 7). The Rim101 transcription factor appears to regulate encapsulation primarily through mediating cell wall changes that render the fungal cell competent to maintain the polysaccharide capsule at its surface (8). Without these adaptive cell wall changes, the *rim101Δ* mutant is unable to maintain the antigen masking provided by the capsule, thus resulting in an excessive inflammatory response by the host (9). Our focus here is to determine the mechanisms of Rim101 activation and effector function that specifically allow *C. neoformans* to survive in the host.

The Rim101/PacC zinc finger transcription factor was first identified in *Saccharomyces cerevisiae* and *Aspergillus nidulans* as a major effector of alkaline pH responses (10, 11). Extracellular pH signals are recognized at the plasma membrane and are transferred to the endosomal membranes through arrestin-like signaling and the ESCRT (endosomal sorting complex required for transport) machinery (12–20). At the endosomal membranes, Rim101 is cleaved at the C terminus and is then localized to the nucleus (21, 22). The members of this pH response pathway are highly conserved and have been identified in most fungal species. The *C. neoformans* genome also contains many elements of this conserved pathway, but there are no obvious homologues of the membrane-associated pH sensors. We propose that, instead, *C. neoformans* Rim101 has additional or alternative activating signals through the cyclic AMP (cAMP)/protein kinase A (PKA) pathway (8).

In *C. neoformans*, Rim101 is important in the regulation of a number of responses to host stresses. In addition to exhibiting altered cell wall composition and defects in the capsule, the *rim101Δ* mutant is sensitive to low iron levels, high salt concentrations, and alkaline pHs (8, 23, 24). Many of these mutant phenotypes are conserved among *rim101Δ* mutants in other fungi, including the pathogens *Candida albicans*, *Aspergillus fumigatus*, and *Ustilago maydis* (25–31). Extensive work with these fungi has also revealed a conserved 5′-GCCAAG-3′ binding motif for the Rim101 transcription factor, allowing the prediction of direct targets that may influence adaptation to external pH signals (32–35).

Previously identified direct targets of Rim101 in *C. albicans* include the cell wall glycosidase genes *PHR1* and *PHR2* and the

TABLE 1 Fold changes in the expression of the *ENA1*, *CTR4*, and *RIM101* genes in strains incubated under various conditions

Strain and condition[b]	Fold change in expression[a] (SEM)		
	ENA1	*CTR4*	*RIM101*
H99			
YPD	1 (0.00)	1 (0.00)	1.00 (0.00)
NaCl	0.52 (0.04)	0.07 (0.05)	0.85 (0.22)
TC	5.86 (0.20)	10.11 (5.35)	3.30 (0.57)
pka1Δ mutant			
YPD	0.84 (0.04)	1.98 (1.38)	0.76 (0.08)
NaCl	1.04 (0.03)	1.26 (0.88)	0.87 (0.00)
TC	6.50 (0.06)	0.51 (0.30)	0.92 (0.02)
rim101Δ mutant			
YPD	0.52 (0.18)	0.27 (0.12)	
NaCl	0.11 (0.00)	0.46 (0.27)	
TC	1.68 (0.90)	5.63 (4.22)	

[a] As determined by RT-PCR.
[b] NaCl, YPD plus 1.5 M NaCl; TC, tissue culture medium.

TABLE 2 Primers used for gel shift assays

Target	Sequences[a]
CFT1 promoter with Rim101 binding site	CAATTTTTGT<u>GCCAAG</u>AATGGAAAG; CTTTCCATT<u>CTTGGC</u>ACAAAAATTG
CIG1 promoter with Rim101 binding site	TCGCTTTTT<u>GCCAAG</u>AACATTGACC; GGTCAATGTT<u>CTTGGC</u>AAAAAGAGA
CIG1 promoter with mutated binding site	TCGCTTTTTGCT<u>GAGAAC</u>ATTGACC; GGTCAAT<u>GTTCTC</u>AGCAAAAAGCGA

[a] The predicted Rim101 binding sites are underlined.

ferric reductase genes *FRE1* and *FRP1* (26, 28, 32, 35). Rim101 activates the expression of both ferric reductases but represses the expression of *PHR2* (34, 35). In *S. cerevisiae*, however, Rim101 acts primarily as a negative regulator of gene expression, and major Rim101 targets include the Nrg1 and Smp1 transcription factors (33). Moreover, Rim101 may bind to promoters in an additive manner; the *A. nidulans ipnA* gene requires PacC/Rim101 binding at all three sites in the promoter for full activation of expression (36). Therefore, although the Rim101 motif is conserved in divergent fungal species, the specific effector genes and the mode of Rim101 regulation appear to differ.

To date, the role of *C. neoformans* Rim101 in transcriptional adaptations to the host has only been inferred from comparative gene expression data. In this work, we demonstrate that the *C. neoformans* Rim101 protein interacts directly with genes that are necessary for adaptation to the host, especially for processes involved in cell wall remodeling and capsule attachment. We hypothesize that the connections between Rim101 and Pka1 in *C. neoformans* allow a wider range of activating signals for the Rim101 transcription factor than in other fungi. Using chromatin immunoprecipitation, we demonstrate that *C. neoformans* Rim101 can act both as an activator and as a repressor of transcription, depending on the target gene. Moreover, we use *in vivo* RNA profiling to examine the transcriptional response of this pathogen to the host. This analysis revealed the limitations of extrapolating results from simple *in vitro* growth conditions and emphasized the importance of examining a pathogen in the context of infection to determine the precise regulatory pathways controlling biologically relevant phenotypes. We propose a model in which *C. neoformans* uses both the cAMP/PKA and pH-sensing pathways to activate Rim101 in response to host signals. Rim101 activation is required for direct regulation of multiple cell wall components. In turn, active cell wall remodeling creates a surface that minimizes the exposure of immunogenic epitopes, favoring fungal cell survival within the host by facilitating immune evasion.

MATERIALS AND METHODS

Strains and media. The *Cryptococcus neoformans* strains used in this study were H99 and the *rim101Δ*, *pka1Δ*, *rim20Δ*, *rim101Δ pHis-GFP-RIM101*,

and *rim101Δ pRim101-GFP-RIM101* strains. Host conditions were approximated *in vitro* using two types of tissue culture medium, CO_2-independent medium and Dulbecco's modified Eagle's medium (DMEM), buffered to pH 7.4. These two media result in similar levels of Rim101 and capsule activation. CO_2-independent tissue culture medium was obtained from Gibco (Invitrogen). An alkaline-pH medium was created by buffering yeast extract-peptone-dextrose (YPD) with 25 mM HEPES and adjusting the medium to the target pH with NaOH. A salt medium was prepared by adding 1.5 M NaCl to YPD.

RNA sequencing and transcript analysis. To determine the transcription changes dependent on the *pka1Δ* mutation, the *pka1Δ* mutant was incubated under conditions identical to those for strains used in prior transcriptome sequencing (RNA-Seq) experiments. Briefly, the cells were incubated in YPD medium to mid-log phase, washed twice, and then incubated for 3 h at 37°C either in DMEM with 5% CO_2 or in YPD. Cells were then washed twice, frozen on dry ice, and lyophilized for 3 h. Total RNA was extracted using the Qiagen RNeasy plant minikit (Qiagen, Valencia, CA), as described previously (8, 9).

All library preparation and RNA sequencing were performed by the Duke Sequencing Core Facility, as described previously (9). The *pka1Δ* mutant was sequenced with 36-bp single-end reads. All reads were mapped to the *C. neoformans* reference genome provided by the Broad Institute by using TopHat, version 1.3.0, as described previously (9, 37). All data were uploaded to the NCBI GEO database. Genes were considered significantly differentially expressed if *P* values were greater than the false discovery rate after Benjamini-Hochberg corrections for multiple testing and if the fold change was greater than 2.0.

RNA extraction, cDNA preparation, and RT-PCR. Strains cultured overnight in YPD at 30°C were diluted in YPD medium alone, YPD medium with 1 M NaCl, or CO_2-independent medium to an optical density at 600 nm (OD_{600}) of 1.0. The strains were cultured under these conditions for 3 h at 30°C with shaking at 150 rpm. Cells were harvested and were flash frozen on dry ice. RNA was purified from lyophilized cells using the Qiagen RNeasy kit for plants and fungi. The Clontech Advantage RT-for-PCR kit was used to make cDNA. Real-time PCR (RT-PCR) was carried out as described previously (38), with an annealing temperature of 60°C. Negative controls without reverse transcriptase were included. The primers used were as follows: for *GPD1*, forward primer AGTATGACTCCACACATGGTCG and reverse primer AGACAAACATCGGAGCATCAGC; for *ENA1*, forward primer GCTCTACTTGCTTTCCGGTA and reverse primer TGTACACGACAGGGAAAGTC; for *CTR4*, forward primer GTCGAATCTCGATGTTGC and reverse primer GGAACATATCGTGGAGC; and for *RIM101*, forward primer TCATCTCGAGTGCACAC and reverse primer ATTATCATGTCTTGGTC. The fold change was calculated against the wild-type sample in YPD by using the Δ^{CT} method, with *GPD1* as the internal control (Table 1).

Gel shift assay. DNA probes for electrophoretic mobility shift assays (EMSAs) were double-stranded synthetic oligonucleotides corresponding to either 15 or 25 nucleotides spanning the putative Rim101 binding site in the *CFT1* promoter. The sequences are given in Table 2.

The mutated probe contained a 5′-GAGAAG-3′ motif instead of the 5′-GCCAAG-3′ motif. Biotin labeling and EMSAs were performed ac-

cording to the manufacturer's instructions (Pierce LightShift chemiluminescent EMSA kit; Thermo Scientific, Rockford, IL, USA). For each lane, 6 μl of protein extract was used. Protein extracts were obtained as described previously (8).

Chromatin immunoprecipitation. Strains were incubated in CO_2-independent tissue culture medium for 3 h and were then cross-linked for 2 h in 1% formaldehyde before quenching with glycine. Chromatin immunoprecipitation was performed as described previously (39), with minor modifications. An antibody against green fluorescent protein (GFP) (Roche) was used to immunoprecipitate the Gfp-Rim101 fusion protein and the associated DNA. A mock-antibody-treated strain and the wild-type strain (without GFP) were used as controls. Enrichment was determined by real-time PCR of candidate promoters, by comparing the immunoprecipitated sample to the mock-antibody control by use of the comparative threshold cycle (C_T) method (40).

Microscopy. Fluorescent images were captured using a DeltaVision Elite deconvolution microscope equipped with a CoolSnap HQ2 high-resolution charge-coupled device (CCD) camera. Cells were cultured either in CO_2-independent medium (pH 7.4) (Gibco) or in YPD (pH 6.0) plus 150 mM HEPES for 4 to 5 h. To visualize nuclei, the Hoechst 33342 nucleic acid stain (Invitrogen) was added to 10 μg/ml and was incubated for 15 min. To minimize background fluorescence, cells were washed and were resuspended in synthetic complete medium (pH 6.0) containing McIlvaine's buffer or in CO_2-independent medium. At an acidic pH, the Hoechst 33342 nuclear stain shows membrane staining (41).

Cell wall analysis. For cell wall staining, strains were first washed and then stained with wheat germ agglutinin (WGA) conjugated to Alexa Fluor 488 (chitin) (Molecular Probes, Eugene, OR) (42, 43). After staining, cells were washed twice before observation by fluorescence microscopy. WGA was observed using a 488-nm wavelength for fluorescence. Images were captured with a Zeiss Axio Imager.A1 fluorescence microscope equipped with an AxioCam MRm digital camera.

***In vivo* RNA profiling.** Female A/J mice were infected with 5×10^5 cells by using the inhalational model of cryptococcal infection, as described previously (9). The mice were sacrificed 4 days postinfection, and the lungs were harvested. Immediately after harvesting, infected lungs were cut into the separate lobes and were flash frozen in dry ice. The frozen lungs were then homogenized by three rounds of 30-s beating on a mini-bead beater using 0.2-μm acid-washed glass beads. RNA was extracted from the tissue homogenate by using the Qiagen RNeasy Plant minikit according to the manufacturer's instructions (Qiagen, Valencia, CA). All animal experiments were performed in accordance with Duke University institutional guidelines for the ethical care of experimental animals.

Fungal gene expression *in vivo* was analyzed by nanoString profiling as described previously (44). Briefly, 10 μg of *C. neoformans*-infected mouse tissue RNA was mixed with a custom-designed probe set and was processed according to the manufacturer's instructions. Six hundred fields per sample were scanned on the nanoString digital analyzer. The raw counts were adjusted for technical variability by using irrelevant RNA sequences included in the code set. The adjusted counts were then normalized to the expression of five housekeeping genes (expressing aldose reductase [CNAG_02722], cofilin [CNAG_02991], microtubule binding protein [CNAG_00816], mitochondrial protein [CNAG_00279], and phosphoglycerate kinase [CNAG_03358]).

RESULTS

Pka1 and Rim101 share downstream targets. In *C. neoformans*, there is evidence that the PKA signaling pathway helps to control Rim101 localization and function. Therefore, we hypothesized that examining the transcriptional profiles of the *rim101Δ* and *pka1Δ* mutants in comparison to that of the wild type would reveal the extent of PKA1 regulation of Rim101 activity (8). To define the overlapping and unique sets of genes with Pka1- and Rim101-dependent transcription, we compared the global transcriptional profiles of the *pka1Δ* and *rim101Δ* mutant strains to that of the wild type (45, 46).

Previously, we performed deep mRNA sequencing of wild-type and *rim101Δ* cells after incubation in tissue culture medium for 3 h (9). This condition results in heat stress, slight pH stress (since *C. neoformans* has a preference for acidic pHs), and altered nutrient availability. We noted that 1,257 genes have significantly different expression in the *rim101Δ* mutant strain and the wild type. We subsequently performed transcriptional analysis of the *pka1Δ* mutant strain incubated under identical conditions. This comparative transcriptional profiling revealed 1,476 genes with at least 2-fold differences in expression between the *pka1Δ* mutant and the wild type (see Table S1 in the supplemental material). Of these, 1,077 genes were common to both sets; these genes demonstrated transcriptional dependence on both Pka1 and Rim101.

To examine the network structure, we performed pairwise correlation analysis of the entire transcriptomes of the *pka1Δ* and *rim101Δ* mutant strains (46). This analysis revealed a strong correlation between Pka1- and Rim101-dependent genes (adjusted r^2, 0.515; P, <0.001). This correlation increased dramatically when we examined only those genes that were at least 2-fold differentially expressed in the wild-type and mutant strains (adjusted r^2, 0.923; P, <0.001). Moreover, the majority of genes with Rim101-dependent expression demonstrated a similar direction and magnitude of transcriptional control by Pka1 (Fig. 1A). This strong correlation between the *rim101Δ* and *pka1Δ* mutant transcriptomes supports our hypothesis that *C. neoformans* Pka1 and Rim101 are in the same intracellular signaling pathway. It also suggests a model in which Pka1 is required for the majority of the Rim101 transcriptional regulation activity (Fig. 1B).

Among the coregulated biological processes, we observed similar differences in the expression of multiple proteins involved in cell wall biosynthesis and remodeling (especially in processes related to α-1,3 glucan, β-1,3 glucan, and β-1,6 glucan synthesis), consistent with previously documented changes in *rim101Δ* cell walls (9). Additionally, 5 of the 7 genes involved in chitin and chitosan biosynthesis (47–50) were differentially expressed in the two mutant strains compared with the wild type.

To further explore the altered cell wall phenotype, we examined chitin localization in the wild-type strain and the *pka1Δ*, *rim101Δ*, and *rim20Δ* mutant strains by using a fluorescently conjugated lectin (fluorescein isothiocyanate [FITC]-conjugated wheat germ agglutinin [WGA]). Rim20 is part of the scaffold that is required for Rim101 cleavage as part of the canonical pH-sensing pathway (51). Each strain was incubated in tissue culture medium for 24 h prior to WGA addition. We observed similar patterns of staining in the *rim101Δ*, *rim20Δ*, and *pka1Δ* mutant strains (Fig. 2A). Unlike the wild-type strain, which shows staining only at the bud necks, the *rim101Δ*, *rim20Δ*, and *pka1Δ* strains show a more diffuse pattern of WGA-associated fluorescence around the entire cell, consistent with similar alterations in cell wall chitin content. These results suggest that cell wall remodeling via Rim101 is dependent on both the pH pathway and the cAMP pathway.

Despite the striking similarities between Pka1- and Rim101-dependent gene expression, several genes were transcriptionally regulated by only one of these proteins. This suggests both Pka1-dependent and Pka1-independent regulation of Rim101. This observation may explain some of the phenotypic differences between the *pka1Δ* and *rim101Δ* mutant strains.

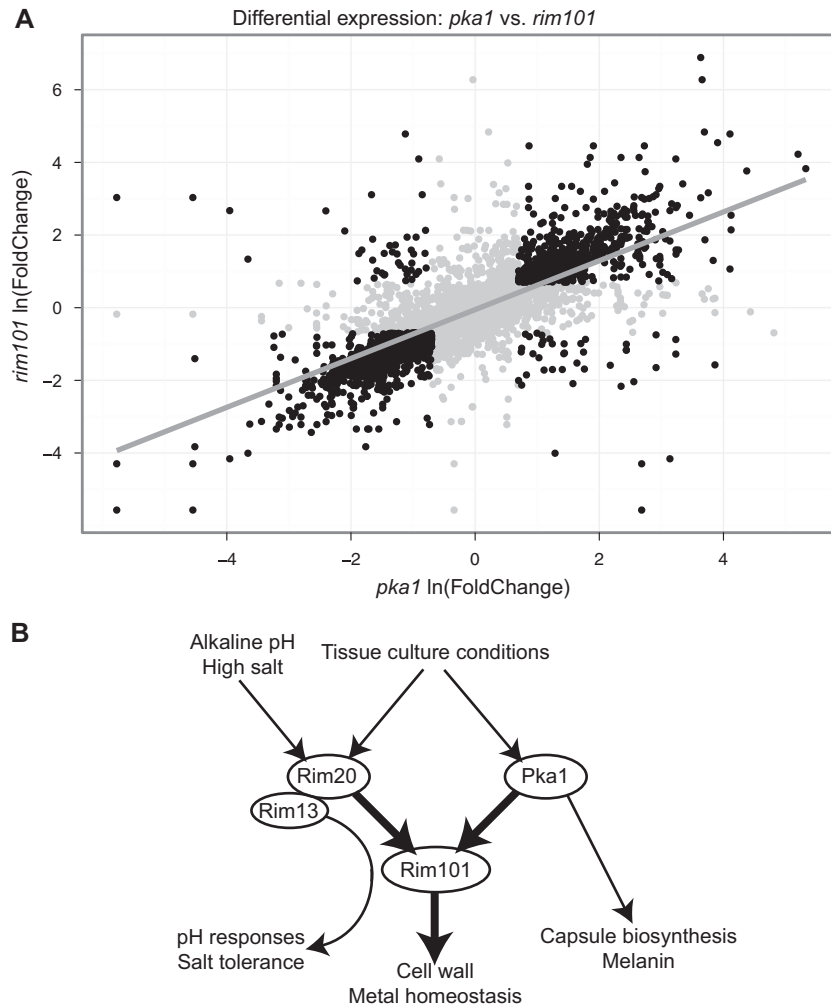**A** Differential expression: *pka1* vs. *rim101*

B

FIG 1 (A) Pairwise correlation analysis of the entire transcriptomes of the *rim101*Δ and *pka1*Δ mutant strains. Gene expression levels for the two mutant strains were determined in comparison with those for the wild-type strain. The transcriptomes of the *pka1*Δ, *rim101*Δ, and wild-type strains were defined using RNA-Seq analysis after incubation in tissue culture medium (DMEM) for 3 h. Shaded circles represent genes that were <2-fold differentially expressed in the wild-type and mutant strains. The adjusted r^2 for the entire transcriptomes was 0.515 (P, <0.001). The adjusted r^2 for the comparison of the significantly differentially expressed genes only was 0.923 (P, <0.001). (B) The concordance between Rim101- and Pka1-dependent gene expression supports a model in which the Rim101 transcription factor is controlled by the classical Rim/pH-responsive pathway (including Rim20 and Rim13) as well as by the cAMP/Pka1 pathway to regulate several cellular processes.

For example, the *ENA1* gene, encoding a sodium transporter, was regulated only by the Rim101 pathway; *rim101*Δ mutant strains failed to support the level of *ENA1* expression that was observed in the wild type and the *pka1*Δ mutant. The functional consequence of this Rim101-Ena1 association is suggested by the observation that both *ena1*Δ and *rim101*Δ mutants fail to grow on media with high concentrations of salt or with a high pH. Additionally, the divergent dependence of Ena1 on Rim101 and Pka1 may explain the phenotypic differences between the sensitivities of the *rim101*Δ and *pka1*Δ mutants to high pHs and high salt concentrations (Fig. 2B) (52). Importantly, the *rim20*Δ mutant shares the salt and pH sensitivities of the *rim101*Δ strain, suggesting that tolerance to alkaline pHs and high salt concentrations is regulated primarily by the Rim/pH-sensing pathway.

To support these findings, we used targeted RT-PCR analysis of *ENA1* expression in YPD, tissue culture medium, and a high-salt medium (Fig. 2C). We observed that *ENA1* expression is

highly induced under these conditions in the wild-type and *pka1*Δ mutant strains but not in the *rim101*Δ mutant. This also suggests that Rim101 is able to induce *ENA1* expression in the absence of Pka1 phosphorylation, presumably through activation by distinct components of the Rim/pH-sensing pathway. Together, these data support an emerging model in which the *C. neoformans* PKA and Rim pathways control overlapping targets regulating cell wall dynamics, as well as distinct targets involved in other cell processes, such as tolerance to different salt concentrations (Fig. 1B).

Rim101 binds a conserved motif. The set of Rim101-dependent genes that we identified through comparative transcriptional profiling is composed of both direct and indirect targets of the Rim101 transcription factor. To determine experimentally the direct targets of Rim101 action, we first investigated whether a previously established Rim101-binding motif from other fungi is conserved in *C. neoformans*. Rim101 homologues in other species bind to the 5′-GCCAAG-3′ motif in the promoters of direct target
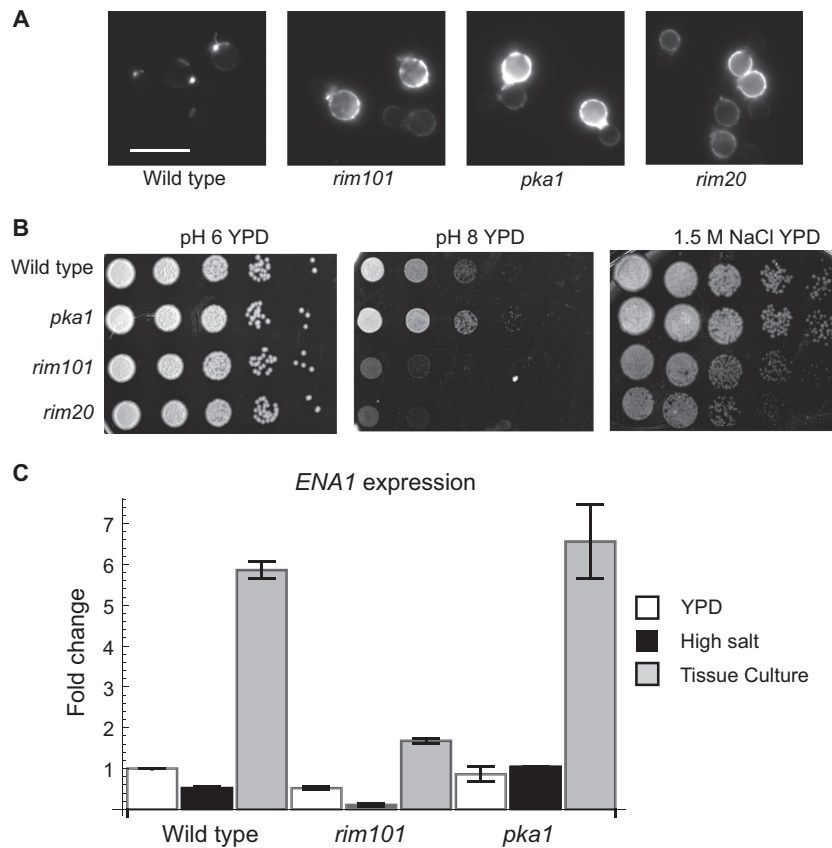
FIG 2 The *rim101Δ* and *pka1Δ* strains have both overlapping and divergent phenotypes. (A) The *rim101Δ* and *pka1Δ* mutants demonstrate similar alterations in WGA binding patterns. Cells were incubated for 24 h in tissue culture medium before staining with FITC-conjugated WGA. All micrographs were taken at the same exposure in order to distinguish the fluorescence levels of the different strains. (B) The *rim101Δ* and *rim20Δ* mutants have defects at an alkaline pH and under high-salt conditions. A total of 1×10^6 cells were 10-fold serially diluted onto plates under the conditions indicated and were incubated at 30°C. (C) *ENA1* shows Rim101- but not Pka1-dependent changes in expression. RNA was extracted from wild-type, *rim101Δ*, and *pka1Δ* strains after incubation for 3 h in a rich medium (YPD), under tissue culture conditions, or with high salt concentrations. *ENA1* transcript levels were determined by quantitative reverse transcriptase PCR. The fold change was calculated relative to wild-type levels in YPD and was normalized to the expression of the internal control, *GPD1*.

genes (30, 32). As reported previously, this putative target sequence is present in the promoters of many genes with Rim101-dependent expression (8). We used electrophoretic mobility shift assays to determine whether *C. neoformans* Rim101 (CnRim101) actually binds this motif. For these experiments, we chose 25-mers spanning the 5′-GCCAAG-3′ motif from the promoter of the *C. neoformans* iron transporter gene *CFT1*, which is highly differentially expressed in the *rim101Δ* and wild-type strains. We observed distinct mobility shifts of the labeled oligomer when it was incubated with protein extracts from the wild-type strain but not with extracts from the *rim101Δ* mutant (Fig. 3A, lane 1 versus lane 2). To determine the specificity of protein binding, we added excess unlabeled 15-mer oligomers containing this motif, and we observed a competitive reversal of the electrophoretic shift (Fig. 3A, lanes 3 and 4). Incubation of the labeled oligomer with protein extracts from the *rim101Δ Gfp-Rim101* strain resulted in a supershift in electrophoretic mobility (Fig. 3B). Together, these data strongly suggest that Rim101 binds directly to the 5′-GCCAAG-3′ motif in this target gene promoter. Additionally, when we incubated protein extracts with a mutated oligomer (5′-GCCAAG-3′ →5′-GAGAAG-3′), we did not observe a shift in mobility, indicating the specificity of interactions of Rim101 with its DNA binding site (Fig. 3C).

Then we analyzed the promoters of the Rim101-regulated genes for the presence of this motif. Of the 1,257 genes differentially regulated by Rim101, 564 had this conserved motif in the 1,000 bp upstream of their ATG start sites. In other fungal species, there is evidence that Rim101 can bind a divergent sequence; for example, *C. albicans* Rim101 binds the 5′-CCAAGAA-3′ motif (35). Indeed, the *CHI22* endochitinase, which demonstrates Rim101-dependent expression, has this divergent motif in the putative promoter region. However, for the most stringent initial analysis, we chose to limit our studies to genes containing the most-conserved Rim101 binding motif. We hypothesized that genes that are direct targets of Rim101 would maintain this specific, functional promoter sequence across the *Cryptococcus* genus, including the sister species *Cryptococcus gattii*. Therefore, we examined the promoter regions of orthologs of the Rim101-regulated genes in *C. gattii* (strain R265). Of the 564 Rim101-regulated genes with promoters containing Rim101 binding sites in *Cryptococcus neoformans* var. *grubii*, 310 maintained this promoter sequence in their *C. gattii* orthologs (Fig. 3D). The majority of genes (76.7%) with Rim101 sites in both *C. neoformans* var. *grubii* and *C. gattii* displayed higher expression in the *rim101Δ* mutant than in the wild type, suggesting that Rim101 may act primarily as a negative regulator of gene expression for its direct targets.

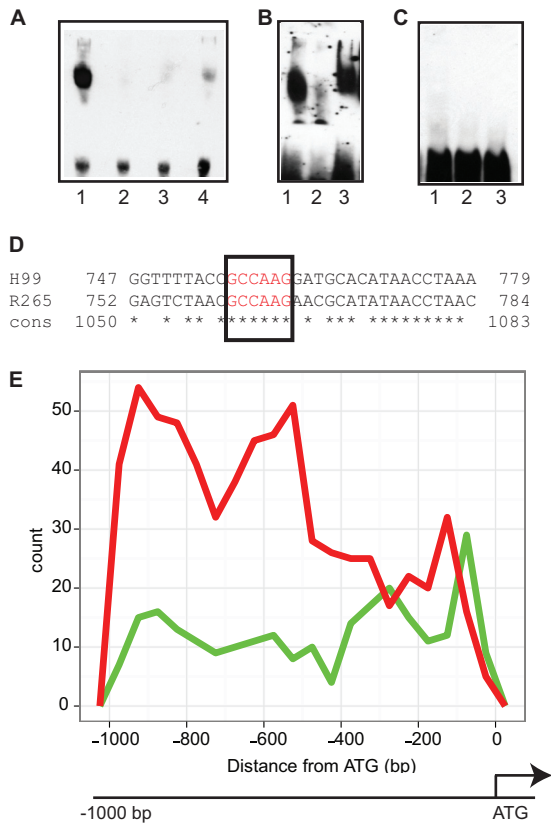We then mapped the position of each potential binding site in

FIG 3 (A to C) Rim101 binds a conserved motif, as determined by EMSAs. (A) A biotin-labeled 25-mer containing the 5′-GCCAAG-3′ motif was incubated with protein extracts from wild-type (lanes 1 and 4) or *rim101Δ* (lanes 2 and 3) cells. The mixtures were assessed by alterations in electrophoretic mobility by PAGE and immunoblotting using streptavidin detection. Excess unlabeled 15-mers were added to lanes 3 and 4. (B and C) A 25-mer containing the 5′-GCCAAG-3′ motif (B) or a mutated Rim101 binding motif (5′-GAGAAG-3′) (C) was incubated with protein extracts from the wild-type (lanes 1), *rim101Δ* (lanes 2), or *rim101Δ/GFP-RIM101* (lanes 3) strain prior to electrophoresis. (D) The promoter of the *ENA1* gene from *C. neoformans* var. *grubii* and its homologous sequence in *C. gattii* were aligned. The conserved Rim101 binding motif is highlighted. Identical nucleotides in a consensus (cons) sequence of this region are indicated by asterisks. (E) Genes with Rim101 binding sites in both *C. neoformans* and *C. gattii* were examined for Rim101-dependent transcription and were separated on the basis of induction (green) or repression (red). The positions of the binding sites were determined, and the number of genes was plotted along a representation of the distance of the Rim101 binding site from the ATG translation start site. All sequences and Rim101 site positions were obtained from FungiDB (www.fungidb.org).

these promoters relative to the ATG site in order to examine whether certain positions were correlated with positive or negative gene regulation (Fig. 3E). This analysis suggested that Rim101 sites that occurred less than 100 bp from the ATG position were associated mainly with Rim101-activated genes. In contrast, Rim101 sites that were approximately 150, 500, or 900 bp upstream of the ATG position were associated mainly with Rim101-repressed genes. The divergence in binding motif position suggests the possibility of interactions between Rim101 and other transcriptional regulators in these promoters, thus allowing a single protein to act as both an activator and a repressor of gene expression.

Rim101 binds a conserved motif *in vivo*. To verify that Rim101 actually binds this conserved motif in the cell, we per-
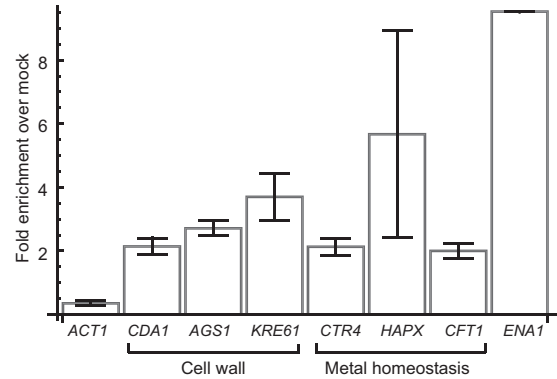

FIG 4 Chromatin immunoprecipitation to detect Gfp-Rim101 DNA binding. Cells were incubated in tissue culture medium for 3 h before fixation and chromatin immunoprecipitation. PCRs were performed using primers that flanked a presumed Rim101 binding site in target gene promoters. The fold change was determined by determining enrichment in the immunoprecipitated sample relative to the no-antibody control. Actin (*ACT1*), which does not contain a Rim101 binding site, was used as a control.

formed chromatin immunoprecipitation after incubating cells under Rim101-activating conditions for 3 h (DMEM tissue culture medium at 37°C). After formaldehyde cross-linking and DNA sonication, we used an anti-GFP antibody to enrich for sequences that were bound to the GFP-Rim101 protein and examined candidate promoters from the subset of Rim101-regulated genes that had Rim101 sites in all species examined. As a control, we examined cells for enrichment at the actin promoter, which does not contain a Rim101 binding site and is not transcriptionally regulated by Rim101.

After incubation under tissue culture conditions for 3 h, we demonstrated enrichment for Rim101 binding at the promoters of three candidate cell wall genes that are among the predicted set of direct targets of Rim101. For *CDA1* and *KRE61*, enrichment for Rim101 binding correlated with an increase in gene expression in the wild-type strain. In contrast, the *AGS1* promoter, which contains a Rim101 binding site 944 bp away from the ATG position, demonstrated 2.8-fold enrichment for Rim101 binding (Fig. 4), as well as higher expression in the *rim101Δ* mutant strain (9). These results suggest that *C. neoformans* Rim101 directly regulates the expression of cell wall genes by binding to their promoters but that the consequences of binding may be modulated by other factors, such as interactions with other proteins and the promoter position of Rim101 binding.

Rim101 has also been implicated in the regulation of iron and copper homeostasis both in *C. neoformans* and in other fungal species (24, 34, 35, 53). Therefore, we examined the Rim101 binding of the promoters of the *HAPX*, *CTR4*, and *CFT1* genes (Fig. 4). Although there was enrichment at all three promoters, *HAPX* demonstrated increased expression in the *rim101Δ* strain, which was consistent with a Rim101 binding motif 519 bp upstream of the ATG site and subsequent Rim101 repression of gene expression. *CTR4* and *CFT1*, with binding sites 279 and 253 bp away, respectively, showed increased expression in the wild-type strain, consistent with activation by Rim101 (Fig. 4). Finally, we examined the binding of Rim101 at the *ENA1* promoter, which also has a conserved Rim101 binding motif. In agreement with the previously discussed phenotypic and gene expression results, we ob-

served striking enrichment for Rim101 binding at the *ENA1* promoter.

nanoString profiling of virulence gene expression *in vitro*. Recently, nanoString RNA profiling has been used to accurately quantify RNA levels in many organisms, including pathogenic fungi such as *C. albicans* (44). This technique avoids the biases introduced during the creation of cDNA libraries for sequencing, and it can be used to compare expression directly across multiple mutant strains and conditions. It has been successfully applied to assess the relative transcript levels of target genes in biological samples. Therefore, we used this methodology to complement our RNA sequencing results and to allow us to examine gene expression under multiple growth conditions.

Taking a targeted approach, we surveyed the expression of 26 genes that were likely to be involved in infection-related processes, such as capsule or melanin induction, metal acquisition, osmotic stress resistance, cell wall remodeling, and pH responses (2). As a control for RNA extraction in each sample, we examined the expression of 5 genes that did not demonstrate variable expression in multiple previous microarray, RNA-Seq, and RT-PCR analyses (8, 24, 54–56). These control genes were chosen to represent a range of absolute expression levels, allowing for the normalization for both weakly and highly expressed genes.

To ensure that the nanoString data would correlate with other methods of transcriptional measurement, we first compared the nanoString data to the RNA-Seq data under *in vitro* growth conditions for the wild-type and *rim101Δ* mutant strains after 3 h of incubation in tissue culture medium. For most genes, we observed a strong concordance with the changes in gene expression that we observed by RNA-Seq and by RT-PCR. However, the RNA-Seq results tended to suggest larger differences in expression (Table 3).

Using nanoString profiling, we were able to distinguish differences in gene expression based both on Rim101 activity and on the incubation condition (Table 4). For example, *ENA1* is strongly induced in the wild-type strain by incubation in CO_2-independent medium. However, the absolute expression levels of this gene are also strongly Rim101 dependent, with 6.7- and 5.9-fold differences in expression between the wild-type and *rim101Δ* mutant strains in a rich medium or CO_2-independent medium, respectively. The expression of *SKN1*, a β-glucan synthase gene, and *CDA1*, a chitin deacetylase, also follows this pattern. In contrast, *KRE6* expression was repressed in a CO_2-independent medium in the wild-type background and was induced in the *rim101Δ* mutant background. Figure 5A displays the normalized RNA counts in the wild-type and *rim101Δ* mutant strains under the two growth conditions for genes that were at least 2-fold differentially expressed in the two strains.

Interestingly, we documented 3.4-fold induction of *RIM101* gene expression in the wild-type strain under tissue culture conditions. The expression of the *RIM101* and *pacC* genes in other fungal species is highly regulated by growth conditions, contributing to the levels of nucleus-localized protein (57). In *C. neoformans*, the *RIM101* gene contains six Rim101 binding motifs in the promoter, suggesting that its expression could be highly autoregulated. The *C. albicans RIM101* promoter contains only two Rim101 binding sites (32). Therefore, we created a Gfp-Rim101 fusion protein expressed under the control of the endogenous promoter (*pRIM101*-Gfp-Rim101) in order to examine the subcellular pattern of protein localization that occurs during growth

TABLE 3 Comparative transcriptional profiling results for selected *C. neoformans* genes in the *rim101* mutant versus the wild type using nanoString and RNA-Seq techniques

Gene product	Gene ID	Fold change in expression (wild type/*rim101* mutant)	
		By nanoString profiling	By RNA-Seq
Cfo1	CNAG_06241	1.02	Below threshold
Ags1	CNAG_03120	0.83	0.49
Cck1	CNAG_00556	0.84	0.39
Cda1	CNAG_05799	2.80	4.78
Cda3	CNAG_01239	0.89	Below threshold
Cdc24	CNAG_04243	0.70	Below threshold
Cft1	CNAG_06242	0.77	2.25
Chs4	CNAG_05581	0.77	0.37
Chs4	CNAG_00546	0.88	0.35
Chs5	CNAG_05818	0.73	1.26
Chs8	CNAG_07499	0.74	0.19
Cir1	CNAG_04864	1.07	0.24
Ctr4	CNAG_00979	1.43	43.16
Ena1	CNAG_00531	5.88	4.67
Fks1	CNAG_06508	0.83	0.15
HapX	CNAG_01242	0.59	0.18
Kre6	CNAG_00914	0.30	0.37
Lrg1	CNAG_05703	0.83	0.28
Ova1	CNAG_02008	0.85	13.36
Pbs2	CNAG_00769	0.81	0.29
pH response regulator Rim9	CNAG_05654	0.57	0.36
Pka1	CNAG_00396	1.03	0.84
Rim101	CNAG_05431		
Skn1	CNAG_00897	2.67	10.08
Sp1	CNAG_00156	0.63	0.24
Ssk2	CNAG_05063	0.76	0.30

under host-mimicking conditions with physiological levels of protein expression.

In contrast to the constitutively nuclear signal of the histone-driven GFP-Rim101 fusion protein, we observed a limited amount of fluorescent signal in cells expressing the *pRIM101-Gfp-RIM101* allele when incubated in rich medium, consistent with the low levels of expression observed by using nanoString profiling. However, when these cells were shifted to a tissue culture medium at 37°C, we observed a clear accumulation of fluorescence in the nucleus by 3 h (Fig. 5B). This observation is consistent with Rim101 transcriptional induction and protein activation under these physiologically relevant growth conditions.

Rim101 regulates expression changes in animal models of infection. A major advantage of nanoString profiling is the ability to examine the low levels of fungus-specific RNA present in the context of a host sample. Therefore, in addition to studying the role of Rim101 in regulating gene expression *in vitro*, we also explored the Rim101-dependent expression of a set of physiologically relevant genes in the setting of a murine cryptococcal lung infection. We used nanoString profiling to examine the changes in expression of a set of *C. neoformans* genes in a murine inhalational model of *C. neoformans* infection. This fungus typically initiates infection in the lung, making this a highly relevant model of human infection. Also, we demonstrated recently that infection with the *rim101Δ* mutant causes a dramatically greater lung inflammatory response than infection with the wild type (9).

TABLE 4 nanoString quantification of transcript abundance[a]

| Gene name | Putative function | Gene ID | Relative transcript abundance in the following strain under the following condition: | | | | | |
			WT in YPD	WT in TC[b]	*rim101* mutant in YPD	*rim101* mutant in TC	WT in lung ($n = 5$)	*rim101* mutant in lung ($n = 5$)
AGS1	Alpha-glucan synthase	CNAG_03120	1,321	1,960	1,400	2,356	1,040	1,418
CCK1	Casein kinase protein	CNAG_00556	589	748	582	894	547	728
CDA1	Chitin deacetylase	CNAG_05799	1,893	3,464	671	1,239	8,110	3,046
CDA3	Chitin deacetylase	CNAG_01239	433	1,619	376	1,830	675	509
CDC24	Rho-family GTPase	CNAG_04243	235	199	264	284	146	196
CFO1	Ferric oxidase	CNAG_06241	373	911	96	889	5,176	5,083
CFT1	High-affinity iron permease	CNAG_06242	1,203	2,295	251	2,963	5,985	5,281
CHS4	Chitin synthase	CNAG_05581	556	672	561	878	1,117	1,457
CHS4	Chitin synthase	CNAG_00546	211	378	221	431	1,310	1,863
CHS5	Chitin synthase	CNAG_05818	254	404	239	555	713	1,189
CHS8	Chitin synthase	CNAG_07499	241	268	229	364	261	425
CIR1	Iron regulator	CNAG_04864	343	364	286	340	799	684
CTR4	Copper transporter	CNAG_00979	2,443	2,025	214	1,418	3,366	8,524
ENA1	Sodium transporter	CNAG_00531	660	4,946	99	841	5,282	2,702
FKS1	Beta-glucan synthase	CNAG_06508	107	153	119	183	623	946
HAPX	Iron transcription factor	CNAG_01242	96	217	76	368	720	1,065
KRE6	Beta-glucan synthase	CNAG_00914	812	348	791	1,147	700	2,291
LRG1	GTPase-activating protein for the PKC pathway	CNAG_05703	104	102	102	122	144	165
OVA1	Putative phosphatidylethanolamine-binding protein	CNAG_02008	890	1,191	702	1,406	3,348	1,927
PBS2	Member of the HOG signaling cascade	CNAG_00769	339	348	311	431	392	544
RIM9	Conserved pH-responsive protein	CNAG_05654	496	376	462	658	2,543	3,712
PKA1	Protein kinase	CNAG_00396	271	323	227	312	235	260
RIM101	Transcription factor	CNAG_05431	36	122	0	1	336	16
SKN1	Beta-glucan synthase	CNAG_00897	1,304	3,980	379	1,490	3,405	3,183
SP1	*CRZ1* transcription factor homologue	CNAG_00156	235	225	194	358	649	773
SSK2	MAPKKK[c]	CNAG_05063	192	150	193	197	88	108

[a] Relative transcript abundance for selected *C. neoformans* genes was quantified using nanoString profiling after incubation under various *in vitro* and *in vivo* conditions.
[b] TC, tissue culture medium.
[c] MAPKKK, mitogen-activated protein kinase kinase kinase.

To examine infection-specific gene expression changes, we extracted total RNA from the lungs of female A/J mice infected with 5×10^5 cells at 4 days postinfection ($n = 5$) (Table 4). We determined the contribution of the Rim101 transcription factor to the infection process by examining RNA levels of the *rim101Δ* mutant in the lung in identical murine infections.

Overall, we found that most of the genes induced by *in vitro* incubation in tissue culture medium were also induced during infection of a mouse lung. However, a number of genes showed altered expression only in the lung, suggesting the limitations of *in vitro* culture conditions in mimicking the host. Some of these infection-specific genes include the chitin synthase-encoding genes *CHS4* and *CHS5*, as well as the β-1,3 glucan synthase gene *FKS1*, all of which are involved in cell wall biosynthesis. Additionally, we observed that the expression of the *RIM101* gene increased in the wild-type strain during infection and was approximately 9.4-fold induced in the lung by day 4 relative to expression in rich medium, and an additional 2.75-fold increased relative to expression under tissue culture conditions.

When we compared the gene expression profiles of wild-type and *rim101Δ* mutant strains in the lungs ($n = 5$), 13 of the 26 genes that we examined were significantly differentially expressed in the two strains (P, <0.05) (Fig. 6). These included several chitin biosynthesis genes and the α-glucan synthase gene *AGS1*. However, only four genes (*CDA1*, *CTR4*, *ENA1*, and *KRE6*) showed at least a 2-fold difference in expression levels between the strains (Fig. 6). Interestingly, only *CTR4* expression and *KRE6* expression were regulated by both Rim101 and Pka1 in our *in vitro* RNA-Seq analysis. Together, these results are consistent with a model in which the Rim101 transcription factor participates directly in cell wall remodeling within the infected host in response to activation from multiple signaling cascades. These cell wall changes are likely due to direct binding of the Rim101 transcription factor to the promoters of target genes controlling the expression of multiple cell wall components. Intact Rim101 signaling *in vivo* results in cell wall changes that promote capsular polysaccharide binding and antigen masking, allowing more-efficient survival within the host.

DISCUSSION

We hypothesized that in *C. neoformans*, the Rim101 transcription factor responds to signals from both the pH-responsive Rim signal transduction cascade and the cAMP/PKA pathway (8). So far, this connection has been proposed only for *Cryptococcus*; in other fungal species, Rim101 activation has not been demonstrated to require phosphorylation by PKA (13, 21, 58). To confirm the connections between the cAMP/PKA pathway and the Rim101 transcription factor, we performed deep RNA sequencing of the *rim101Δ* and *pka1Δ* mutants in comparison to the wild-type strain after incubation under tissue culture conditions. Compar-
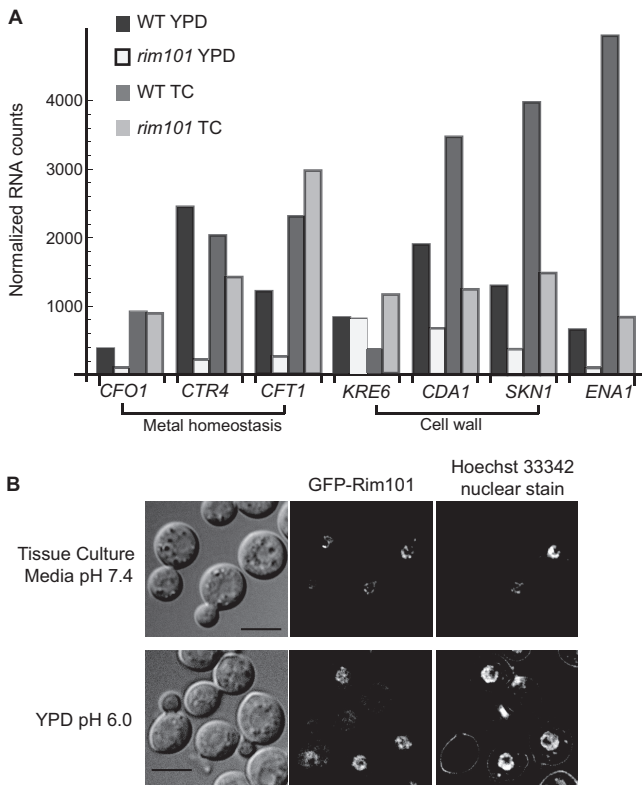
FIG 5 Differences in gene expression and localization due to induction in tissue culture medium. (A) Normalized RNA levels of genes with differential expression in the wild-type and *rim101*Δ mutant strains. Strains were grown in YPD or under tissue culture (TC) conditions for 3 h before RNA extraction. RNA levels were determined by nanoString profiling. RNA levels were normalized to those of control genes as described in Materials and Methods. (B) Rim101 shows increased nuclear localization in tissue culture medium. Cells containing the Gfp-Rim101 fusion protein expressed under the control of the endogenous promoter were incubated in YPD medium (pH 6.0) or in tissue culture medium. Nuclei were stained using the Hoechst 33342 nucleic acid stain.

ison of the downstream transcriptional responses to the *rim101*Δ and *pka1*Δ mutations revealed a striking degree of coordinated gene regulation, providing further evidence for a functional relationship between these genes. Integration of these two pathways appears to give Rim101 flexibility in the upstream signals that allow for activation. Instead of acting primarily as a pH response factor, *C. neoformans* Rim101 can respond to multiple host stimuli via the cAMP/PKA pathway, including such diverse signals as low iron levels or tissue culture medium (59).

This analysis also revealed some targets that demonstrated divergent regulation in the two mutant strains, including genes related to salt and pH sensitivity (52, 60–62). Although it is clear that the Pka1 kinase has multiple downstream targets, the identification of apparently Pka1 independent and Rim101 specific targets raises intriguing questions about alternative mechanisms for the activation of the Rim101 transcription factor.

The overlapping but partially divergent phenotypes of the *rim101*Δ and *pka1*Δ mutants contrast with the absolutely identical phenotypes of the *rim101*Δ mutant and a strain with a mutation in the *RIM20* gene. Rim20 is a member of the conserved pH-sensing pathway, and it acts as a scaffold for Rim101 cleavage and activation (51). This suggests that *C. neoformans* Rim101 activation maintains dependence on the conserved, upstream, pH-responsive signaling elements, even though the expected pH-sensing membrane receptors are not clearly present in the *C. neoformans* genome. In contrast to other fungi for which the pH response has been studied, *C. neoformans* has a strong preference for acidic pHs and a defect in growth above pH 7.4, potentially due to alterations in the upstream members of the pH response pathway.

Despite the divergence in Rim101 activation in *C. neoformans*, there is significant conservation in the downstream targets of Rim101. One of the major cellular processes regulated by Rim101 is the remodeling of the cell wall in response to host signals. We demonstrated previously the importance of this remodeling in the wild-type strain as a mechanism for evading the host immune
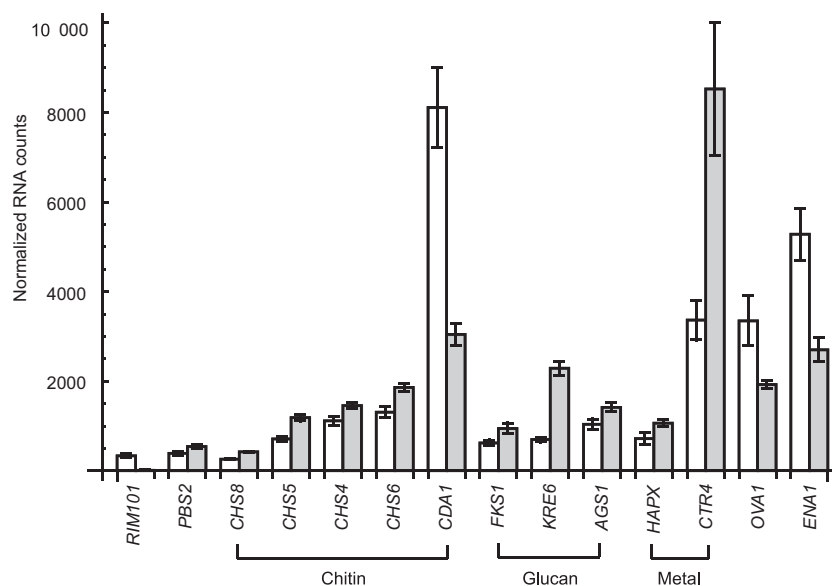

FIG 6 *In vivo* profiling of gene expression. RNA was harvested from mouse lungs (from 5 mice for each strain) infected with either the wild-type (open bars) or the *rim101*Δ mutant (shaded bars) strain. Expression levels were determined by nanoString profiling of candidate genes. The graph includes all genes with significantly different expression in the wild-type and *rim101*Δ strains (*P*, <0.05).

responses ([9]). In many other fungi, Rim101 also regulates cell wall processes. For example, *C. albicans* uses Rim101 to allow for the yeast-hypha transition in response to neutral/alkaline pHs, which is a vital step for tissue invasion and virulence ([63], [64]). Additionally, the *C. albicans* Rim101 pathway regulates the levels of chitin in the cell ([21]). The *S. cerevisiae* Rim101 transcription factor is also required for cell wall assembly, and the *U. maydis* Rim101 transcription factor modulates cell wall sensitivity to lytic enzymes ([25], [65]). Using transcriptional profiling and cell wall staining, we demonstrated previously that *C. neoformans* Rim101 also regulates these genes ([9]). Here we show that the cell wall of the *pka1*Δ mutant has features similar to those of the *rim101*Δ mutant, and many cell wall genes are also differentially regulated in the wild-type and *pka1*Δ mutant strains.

A potential mechanism for this conservation in Rim101 functions is the conservation of the binding motif across these fungal species. Using EMSAs and chromatin immunoprecipitation, we demonstrated that the *C. neoformans* Rim101 protein binds the 5′-GCCAAG-3′ motif, which had been documented previously in *Aspergillus*, *Candida*, and *Saccharomyces* species ([32], [33], [36]). Presumably, the upstream rewiring of the Rim101 activating signal allows *C. neoformans* to induce the expression of a conserved suite of Rim101 targets, such as those involved in cell wall modification, in response to a wider range of activating signals.

In this work, we also observed that Rim101 binding was not completely associated with either induction or repression of the target genes, suggesting that there is interplay between Rim101 and other transcription factors in these promoter regions. In *A. nidulans*, the *gabA* promoter contains overlapping Rim101 and IntA binding sites, resulting in competition for binding and transcriptional regulation ([66]). Both Rim101 and a CBF binding factor control the expression of the *C. albicans FRP1* ferric reductase ([34]). A *C. neoformans* ferric reductase transmembrane component (CNAG_06821) promoter also contains both a Rim101 binding site and a CCAAT motif, suggesting that this gene could be regulated both by Rim101 and by a CBF protein.

Finally, we were able to use nanoString profiling to examine the transcriptional responses to the host. This technology allows for direct quantification of fungal RNA levels within the context of the infected tissue—in our case, the mouse lung. We first confirmed that nanoString profiling recapitulates the *in vitro* transcriptional profiling of cells incubated either in rich medium or under tissue culture conditions.

We were then able to use nanoString profiling to examine fungal gene expression in the mouse lung. This *in vivo* analysis revealed the inadequacies of extrapolating results from *in vitro* growth conditions, since many genes showed a much higher degree of induction in the mouse lung than in tissue culture medium. This is likely due to the large number of stresses in the host that are not completely recapitulated under *in vitro* culture conditions, including interactions with the host immune system or deprivation of particular nutrients. For example, *HAPX*, a gene encoding an important regulator of iron homeostasis, was 2.2-fold differentially regulated in YPD and tissue culture medium but 7.5-fold differentially regulated in YPD and the mouse lung. Furthermore, only 7 of the 26 candidate genes were differentially regulated in YPD and tissue culture medium in the wild-type strain. When YPD expression was compared to *in vivo* expression, 17 of the 26 genes were differentially expressed. The genes with infection-specific induction or repression included the cell wall biosynthesis genes *CDA1*, *CHS4*, *CHS6*, and *FKS1* and the iron genes *CIR1* and *CFT1*.

We were also able to examine the transcriptional profile of the *rim101*Δ mutant and the wild-type strain under host conditions. The major differences in expression between the strains were in the *CDA1*, *KRE6*, *CTR4*, and *ENA1* genes. The *CDA1* gene regulates chitosan levels in the cell, and *KRE6* is involved in β-glucan synthesis, consistent with the role of Rim101 in the regulation of cell wall remodeling. *ENA1* is also required for full proliferation within the cerebrospinal fluid (CSF), although we have not observed a difference in neurotropism or proliferation in the CSF between the *rim101*Δ mutant and the wild type ([67]). Interestingly, the wild-type strain expressed more *CTR4* transcripts than the *rim101*Δ strain under both *in vitro* growth conditions but 2.5-fold fewer in the context of the host lung. This suggests that Rim101 is required for *CTR4* induction during infection but is dispensable during *in vitro* growth. These results emphasize the importance of using animal models to accurately assess disease processes, since *in vitro* assays may not be able to replicate the host conditions fully. Induction of *CTR4* transcripts during lung infections was recently demonstrated by luciferase assays, suggesting that this may be an important factor during infection ([68]).

In conclusion, we propose that *C. neoformans* has integrated cAMP signaling in the activation of a conserved cell wall-regulating transcription factor to allow for active remodeling of the host-pathogen interface during infection. Since *C. neoformans* is an effective intracellular pathogen, this may reflect the need to respond to host conditions in addition to extracellular, alkaline pH signals. By assaying gene expression during infection, we could observe the importance of actively regulating cell surface changes to allow for colonization and pathogenesis.

In *C. neoformans*, induction of the polysaccharide capsule is a major component of virulence. In these studies, we demonstrate that other cell surface components, including chitin and chitosan, α-glucan, and β-glucan, are also highly regulated during infection. Our profiling data support previous characterizations of host responses in illustrating a role for Rim101-responsive gene expression during lung infection and in identifying cell wall genes among the *in vivo* Rim101 targets. Moreover, the strong induction of Rim101 transcripts in the host lung suggests that Rim101 is a major regulator of these phenotypes.

ACKNOWLEDGMENTS

REFERENCES

1. **Alspaugh J, Perfect J, Heitman J.** 1998. Signal transduction pathways regulating differentiation and pathogenicity of *Cryptococcus neoformans*. Fungal Genet. Biol. **25**:1–14. http://dx.doi.org/10.1006/fgbi.1998.1079.
2. **O'Meara TR, Alspaugh JA.** 2012. The *Cryptococcus neoformans* capsule: a sword and a shield. Clin. Microbiol. Rev. **25**:387–408. http://dx.doi.org/10.1128/CMR.00001-12.
3. **Dykstra MA, Friedman L, Murphy JW.** 1977. Capsule size of *Cryptococcus neoformans*: control and relationship to virulence. Infect. Immun. **16**:129–135.
4. **Kozel T, Gotschlich E.** 1982. The capsule of *Cryptococcus neoformans* passively inhibits phagocytosis of the yeast by macrophages. J. Immunol. **129**:1675–1680.

5. **Chang YC, Kwon-Chung KJ.** 1994. Complementation of a capsule-deficient mutation of *Cryptococcus neoformans* restores its virulence. Mol. Cell. Biol. **14:**4912–4919.

6. **Chang YC, Penoyer LA, Kwon-Chung KJ.** 1996. The second capsule gene of *Cryptococcus neoformans*, *CAP64*, is essential for virulence. Infect. Immun. **64:**1977–1983.

7. **Doering TL.** 2009. How sweet it is! Cell wall biogenesis and polysaccharide capsule formation in *Cryptococcus neoformans*. Annu. Rev. Microbiol. **63:**223–247. http://dx.doi.org/10.1146/annurev.micro.62.081307.162753.

8. **O'Meara TR, Norton D, Price MS, Hay C, Clements MF, Nichols CB, Alspaugh JA.** 2010. Interaction of *Cryptococcus neoformans* Rim101 and protein kinase A regulates capsule. PLoS Pathog. **6:**e1000776. http://dx.doi.org/10.1371/journal.ppat.1000776.

9. **O'Meara TR, Holmer SM, Selvig K, Dietrich F, Alspaugh JA.** 2013. *Cryptococcus neoformans* Rim101 is associated with cell wall remodeling and evasion of the host immune responses. mBio **4**(1):e00522–12. http://dx.doi.org/10.1128/mBio.00522-12.

10. **Caddick MX, Brownlee AG, Arst HN.** 1986. Regulation of gene expression by pH of the growth medium in *Aspergillus nidulans*. Mol. Gen. Genet. **203:**346–353. http://dx.doi.org/10.1007/BF00333978.

11. **Su SSY, Mitchell AP.** 1993. Molecular characterization of the yeast meiotic regulatory gene *RIM1*. Nucleic Acids Res. **21:**3789–3797. http://dx.doi.org/10.1093/nar/21.16.3789.

12. **Li W, Mitchell AP.** 1997. Proteolytic activation of Rim1p, a positive regulator of yeast sporulation and invasive growth. Genetics **145:**63–73.

13. **Lamb T, Xu W, Diamond A, Mitchell AP.** 2001. Alkaline response genes of *Saccharomyces cerevisiae* and their relationship to the RIM101 pathway. J. Biol. Chem. **276:**1850–1856. http://dx.doi.org/10.1074/jbc.M008381200.

14. **Herranz S, Rodriguez JM, Bussink H-J, Sanchez-Ferrero JC, Arst HN, Jr, Penalva MA, Vincent O.** 2005. Arrestin-related proteins mediate pH signaling in fungi. Proc. Natl. Acad. Sci. U. S. A. **102:**12141–12146. http://dx.doi.org/10.1073/pnas.0504776102.

15. **Calcagno-Pizarelli AM, Negrete-Urtasun S, Denison SH, Rudnicka JD, Bussink H-J, Munera-Huertas T, Stanton L, Hervás-Aguilar A, Espeso EA, Tilburn J, Arst HN, Jr, Peñalva MA.** 2007. Establishment of the ambient pH signaling complex in *Aspergillus nidulans*: PalI assists plasma membrane localization of PalH. Eukaryot. Cell **6:**2365–2375. http://dx.doi.org/10.1128/EC.00275-07.

16. **Galindo A, Hervás-Aguilar A, Rodríguez-Galán O, Vincent O, Arst HN, Jr, Tilburn J, Peñalva MA.** 2007. PalC, one of two Bro1 domain proteins in the fungal pH signalling pathway, localizes to cortical structures and binds Vps32. Traffic **8:**1346–1364. http://dx.doi.org/10.1111/j.1600-0854.2007.00620.x.

17. **Cornet M, Bidard F, Schwarz P, Da Costa G, Blanchin-Roland S, Dromer F, Gaillardin C.** 2005. Deletions of endocytic components VPS28 and VPS32 affect growth at alkaline pH and virulence through both RIM101-dependent and RIM101-independent pathways in *Candida albicans*. Infect. Immun. **73:**7977–7987. http://dx.doi.org/10.1128/IAI.73.12.7977-7987.2005.

18. **Hayashi M, Fukuzawa T, Sorimachi H, Maeda T.** 2005. Constitutive activation of the pH-responsive Rim101 pathway in yeast mutants defective in late steps of the MVB/ESCRT pathway. Mol. Cell. Biol. **25:**9478–9490. http://dx.doi.org/10.1128/MCB.25.21.9478-9490.2005.

19. **Rothfels K, Tanny JC, Molnar E, Friesen H, Commisso C, Segall J.** 2005. Components of the ESCRT pathway, DFG16, and YGR122w are required for Rim101 to act as a corepressor with Nrg1 at the negative regulatory element of the *DIT1* gene of *Saccharomyces cerevisiae*. Mol. Cell. Biol. **25:**6772–6788. http://dx.doi.org/10.1128/MCB.25.15.6772-6788.2005.

20. **Herrador A, Herranz S, Lara D, Vincent O.** 2010. Recruitment of the ESCRT machinery to a putative seven-transmembrane-domain receptor is mediated by an arrestin-related protein. Mol. Cell. Biol. **30:**897–907. http://dx.doi.org/10.1128/MCB.00132-09.

21. **Li M, Martin SJ, Bruno VM, Mitchell AP, Davis DA.** 2004. *Candida albicans* Rim13p, a protease required for Rim101p processing at acidic and alkaline pHs. Eukaryot. Cell **3:**741–751. http://dx.doi.org/10.1128/EC.3.3.741-751.2004.

22. **Mingot JM, Espeso EA, Diez E, Penalva MA.** 2001. Ambient pH signaling regulates nuclear localization of the *Aspergillus nidulans* PacC transcription factor. Mol. Cell. Biol. **21:**1688–1699. http://dx.doi.org/10.1128/MCB.21.5.1688-1699.2001.

23. **Cadieux B, Lian T, Hu G, Wang J, Biondo C, Teti G, Liu V, Murphy MEP, Creagh AL, Kronstad JW.** 2013. The mannoprotein Cig1 supports iron acquisition from heme and virulence in the pathogenic fungus *Cryptococcus neoformans*. J. Infect. Dis. **207:**1339–1347. http://dx.doi.org/10.1093/infdis/jit029.

24. **Jung WH, Saikia S, Hu G, Wang J, Fung CK-Y, D'Souza C, White R, Kronstad JW.** 2010. HapX positively and negatively regulates the transcriptional response to iron deprivation in *Cryptococcus neoformans*. PLoS Pathog. **6:**e1001209. http://dx.doi.org/10.1371/journal.ppat.1001209.

25. **Aréchiga-Carvajal E, Ruiz-Herrera J.** 2005. The RIM101/*pacC* homologue from the basidiomycete *Ustilago maydis* is functional in multiple pH-sensitive phenomena. Eukaryot. Cell **4:**999–1008. http://dx.doi.org/10.1128/EC.4.6.999-1008.2005.

26. **Davis D, Wilson RB, Mitchell AP.** 2000. RIM101-dependent and -independent pathways govern pH responses in *Candida albicans*. Mol. Cell. Biol. **20:**971–978. http://dx.doi.org/10.1128/MCB.20.3.971-978.2000.

27. **Davis D.** 2003. Adaptation to environmental pH in *Candida albicans* and its relation to pathogenesis. Curr. Genet. **44:**1–7. http://dx.doi.org/10.1007/s00294-003-0415-2.

28. **Bensen E, Martin SJ, Li M, Berman J, Davis DA.** 2004. Transcriptional profiling in *Candida albicans* reveals new adaptive responses to extracellular pH and functions for Rim101p. Mol. Microbiol. **54:**1335–1351. http://dx.doi.org/10.1111/j.1365-2958.2004.04350.x.

29. **Espeso EA, Tilburn J, Arst HN, Jr, Penalva MA.** 1993. pH regulation is a major determinant in expression of a fungal penicillin biosynthetic gene. EMBO J. **12:**3947–3956.

30. **Tilburn J, Sarkar S, Widdick DA, Espeso EA, Orejas M, Mungroo J, Penalva MA, Arst HN, Jr.** 1995. The *Aspergillus* PacC zinc finger transcription factor mediates regulation of both acid- and alkaline-expressed genes by ambient pH. EMBO J. **14:**779–790.

31. **Peñalva MA, Tilburn J, Bignell E, Arst HN, Jr.** 2008. Ambient pH gene regulation in fungi: making connections. Trends Microbiol. **16:**291–300. http://dx.doi.org/10.1016/j.tim.2008.03.006.

32. **Ramón AM, Fonzi WA.** 2003. Diverged binding specificity of Rim101p, the *Candida albicans* ortholog of PacC. Eukaryot. Cell **2:**718–728. http://dx.doi.org/10.1128/EC.2.4.718-728.2003.

33. **Lamb TM, Mitchell AP.** 2003. The transcription factor Rim101p governs ion tolerance and cell differentiation by direct repression of the regulatory genes *NRG1* and *SMP1* in *Saccharomyces cerevisiae*. Mol. Cell. Biol. **23:**677–686. http://dx.doi.org/10.1128/MCB.23.2.677-686.2003.

34. **Baek Y, Li M, Davis D.** 2008. *Candida albicans* ferric reductases are differentially regulated in response to distinct forms of iron limitation by the Rim101 and CBF transcription factors. Eukaryot. Cell **7:**1168–1179. http://dx.doi.org/10.1128/EC.00108-08.

35. **Baek Y-U, Martin SJ, Davis DA.** 2006. Evidence for novel pH-dependent regulation of *Candida albicans* Rim101, a direct transcriptional repressor of the cell wall beta-glycosidase Phr2. Eukaryot. Cell **5:**1550–1559. http://dx.doi.org/10.1128/EC.00088-06.

36. **Espeso EA, Penalva MA.** 1996. Three binding sites for the *Aspergillus nidulans* PacC zinc-finger transcription factor are necessary and sufficient for regulation by ambient pH of the isopenicillin N synthase gene promoter. J. Biol. Chem. **271:**28825–28830. http://dx.doi.org/10.1074/jbc.271.46.28825.

37. **Trapnell C, Pachter L, Salzberg SL.** 2009. TopHat: discovering splice junctions with RNA-Seq. Bioinformatics **25:**1105–1111. http://dx.doi.org/10.1093/bioinformatics/btp120.

38. **Cramer KL, Gerrald QD, Nichols CB, Price MS, Alspaugh JA.** 2006. Transcription factor Nrg1 mediates capsule formation, stress response, and pathogenesis in *Cryptococcus neoformans*. Eukaryot. Cell **5:**1147–1156. http://dx.doi.org/10.1128/EC.00145-06.

39. **Chun CD, Brown JCS, Madhani HD.** 2011. A major role for capsule-independent phagocytosis-inhibitory mechanisms in mammalian infection by *Cryptococcus neoformans*. Cell Host Microbe **9:**243–251. http://dx.doi.org/10.1016/j.chom.2011.02.003.

40. **Schmittgen TD, Livak KJ.** 2008. Analyzing real-time PCR data by the comparative C_T method. Nat. Protoc. **3:**1101–1108. http://dx.doi.org/10.1038/nprot.2008.73.

41. **Chang YC, Lamichhane AK, Kwon-Chung KJ.** 2012. Role of actin-bundling protein Sac6 in growth of *Cryptococcus neoformans* at low oxygen concentration. Eukaryot. Cell **11:**943–951. http://dx.doi.org/10.1128/EC.00120-12.

42. **Shedletzky E, Unger C, Delmer DP.** 1997. A microtiter-based fluorescence assay for (1,3)-β-glucan synthases. Anal. Biochem. **249:**88–93. http://dx.doi.org/10.1006/abio.1997.2162.

43. **Fox DS, Cox GM, Heitman J.** 2003. Phospholipid-binding protein Cts1 controls septation and functions coordinately with calcineurin in *Crypto-*

coccus neoformans. Eukaryot. Cell **2**:1025–1035. http://dx.doi.org/10.1128/EC.2.5.1025-1035.2003.

44. **Fanning S, Xu W, Solis N, Woolford CA, Filler SG, Mitchell AP.** 2012. Divergent targets of *Candida albicans* biofilm regulator Bcr1 *in vitro* and *in vivo*. Eukaryot. Cell **11**:896–904. http://dx.doi.org/10.1128/EC.00103-12.

45. **Boj SF, Petrov D, Ferrer J.** 2010. Epistasis of transcriptomes reveals synergism between transcriptional activators Hnf1a and Hnf4a. PLoS Genet. **6**:e1000970. http://dx.doi.org/10.1371/journal.pgen.1000970.

46. **Fanning S, Xu W, Beaurepaire C, Suhan JP, Nantel A, Mitchell AP.** 2012. Functional control of the *Candida albicans* cell wall by catalytic protein kinase A subunit Tpk1. Mol. Microbiol. **86**:284–302. http://dx.doi.org/10.1111/j.1365-2958.2012.08193.x.

47. **Baker LG, Specht CA, Donlin MJ, Lodge JK.** 2007. Chitosan, the deacetylated form of chitin, is necessary for cell wall integrity in *Cryptococcus neoformans*. Eukaryot. Cell **6**:855–867. http://dx.doi.org/10.1128/EC.00399-06.

48. **Baker LG, Specht CA, Lodge JK.** 2009. Chitinases are essential for sexual development but not vegetative growth in *Cryptococcus neoformans*. Eukaryot. Cell **8**:1692–1705. http://dx.doi.org/10.1128/EC.00227-09.

49. **Baker LG, Specht CA, Lodge JK.** 2011. Cell wall chitosan is necessary for virulence in the opportunistic pathogen *Cryptococcus neoformans*. Eukaryot. Cell **10**:1264–1268. http://dx.doi.org/10.1128/EC.05138-11.

50. **Banks IR, Specht CA, Donlin MJ, Gerik KJ, Levitz SM, Lodge JK.** 2005. A chitin synthase and its regulator protein are critical for chitosan production and growth of the fungal pathogen *Cryptococcus neoformans*. Eukaryot. Cell **4**:1902–1912. http://dx.doi.org/10.1128/EC.4.11.1902-1912.2005.

51. **Xu W, Mitchell AP.** 2001. Yeast PalA/AIP1/Alix homolog Rim20p associates with a PEST-like region and is required for its proteolytic cleavage. J. Bacteriol. **183**:6917–6923. http://dx.doi.org/10.1128/JB.183.23.6917-6923.2001.

52. **Idnurm A, Walton FJ, Floyd A, Reedy JL, Heitman J.** 2009. Identification of *ENA1* as a virulence gene of the human pathogenic fungus *Cryptococcus neoformans* through signature-tagged insertional mutagenesis. Eukaryot. Cell **8**:315–326. http://dx.doi.org/10.1128/EC.00375-08.

53. **Jung WH, Sham A, Lian T, Singh A, Kosman DJ, Kronstad JW.** 2008. Iron source preference and regulation of iron uptake in *Cryptococcus neoformans*. PLoS Pathog. **4**:e45. http://dx.doi.org/10.1371/journal.ppat.0040045.

54. **O'Meara TR, Hay C, Price MS, Giles S, Alspaugh JA.** 2010. *Cryptococcus neoformans* histone acetyltransferase Gcn5 regulates fungal adaptation to the host. Eukaryot. Cell **9**:1193–1202. http://dx.doi.org/10.1128/EC.00098-10.

55. **Ko Y-J, Yu YM, Kim G-B, Lee G-W, Maeng PJ, Kim S, Floyd A, Heitman J, Bahn Y-S.** 2009. Remodeling of global transcription patterns of *Cryptococcus neoformans* genes mediated by the stress-activated HOG signaling pathways. Eukaryot. Cell **8**:1197–1217. http://dx.doi.org/10.1128/EC.00120-09.

56. **Haynes BC, Skowyra ML, Spencer SJ, Gish SR, Williams M, Held EP, Brent MR, Doering TL.** 2011. Toward an integrated model of capsule regulation in *Cryptococcus neoformans*. PLoS Pathog. **7**:e1002411. http://dx.doi.org/10.1371/journal.ppat.1002411.

57. **Caracuel Z, Roncero MIG, Espeso EA, González-Verdejo CI, García-Maceira FI, Di Pietro A.** 2003. The pH signalling transcription factor PacC controls virulence in the plant pathogen *Fusarium oxysporum*. Mol. Microbiol. **48**:765–779. http://dx.doi.org/10.1046/j.1365-2958.2003.03465.x.

58. **Peñas MM, Hervas-Aguilar A, Munera-Huertas T, Reoyo E, Penalva MA, Arst HN, Jr, Tilburn J.** 2007. Further characterization of the signaling proteolysis step in the *Aspergillus nidulans* pH signal transduction pathway. Eukaryot. Cell **6**:960–970. http://dx.doi.org/10.1128/EC.00047-07.

59. **Pukkila-Worley R, Gerrald QD, Kraus PR, Boily M-J, Davis MJ, Giles SS, Cox GM, Heitman J, Alspaugh JA.** 2005. Transcriptional network of multiple capsule and melanin genes governed by the *Cryptococcus neoformans* cyclic AMP cascade. Eukaryot. Cell **4**:190–201. http://dx.doi.org/10.1128/EC.4.1.190-201.2005.

60. **Jung K-W, Strain AK, Nielsen K, Jung K-H, Bahn Y-S.** 2012. Two cation transporters Ena1 and Nha1 cooperatively modulate ion homeostasis, antifungal drug resistance, and virulence of *Cryptococcus neoformans* via the HOG pathway. Fungal Genet. Biol. **49**:332–345. http://dx.doi.org/10.1016/j.fgb.2012.02.001.

61. **D'Souza CA, Alspaugh JA, Yue C, Harashima T, Cox GM, Perfect JR, Heitman J.** 2001. Cyclic AMP-dependent protein kinase controls virulence of the fungal pathogen *Cryptococcus neoformans*. Mol. Cell. Biol. **21**:3179–3191. http://dx.doi.org/10.1128/MCB.21.9.3179-3191.2001.

62. **Hu G, Steen BR, Lian T, Sham AP, Tam N, Tangen KL, Kronstad JW.** 2007. Transcriptional regulation by protein kinase A in *Cryptococcus neoformans*. PLoS Pathog. **3**:e42. http://dx.doi.org/10.1371/journal.ppat.0030042.

63. **Nobile CJ, Solis N, Myers CL, Fay AJ, Deneault J-S, Nantel A, Mitchell AP, Filler SG.** 2008. *Candida albicans* transcription factor Rim101 mediates pathogenic interactions through cell wall functions. Cell. Microbiol. **10**:2180–2196. http://dx.doi.org/10.1111/j.1462-5822.2008.01198.x.

64. **Villar CC, Kashleva H, Nobile CJ, Mitchell AP, Dongari-Bagtzoglou A.** 2007. Mucosal tissue invasion by *Candida albicans* is associated with E-cadherin degradation, mediated by transcription factor Rim101p and protease Sap5p. Infect. Immun. **75**:2126–2135. http://dx.doi.org/10.1128/IAI.00054-07.

65. **Castrejon F, Gomez A, Sanz M, Duran A, Roncero C.** 2006. The RIM101 pathway contributes to yeast cell wall assembly and its function becomes essential in the absence of mitogen-activated protein kinase Slt2p. Eukaryot. Cell **5**:507–517. http://dx.doi.org/10.1128/EC.5.3.507-517.2006.

66. **Espeso EA, Arst HN.** 2000. On the mechanism by which alkaline pH prevents expression of an acid-expressed gene. Mol. Cell. Biol. **20**:3355–3363. http://dx.doi.org/10.1128/MCB.20.10.3355-3363.2000.

67. **Lee A, Toffaletti DL, Tenor J, Soderblom EJ, Thompson JW, Moseley MA, Price M, Perfect JR.** 2010. Survival defects of *Cryptococcus neoformans* mutants exposed to human cerebrospinal fluid result in attenuated virulence in an experimental model of meningitis. Infect. Immun. **78**:4213–4225. http://dx.doi.org/10.1128/IAI.00551-10.

68. **Ding C, Festa RA, Chen Y-L, Espart A, Palacios O, Espin J, Capdevila M, Atrian S, Heitman J, Thiele DJ.** 2013. *Cryptococcus neoformans* copper detoxification machinery is critical for fungal virulence. Cell Host Microbe **13**:265–276. http://dx.doi.org/10.1016/j.chom.2013.02.002.